

Catalytic and Thermal 1,2-Rearrangement of (α -Mercaptobenzyl)trimethylsilane

Jie Zhang,[†] Mengzhong Cui,[‡] Shengyu Feng,[†] Xiaomin Sun,^{§,||} and Dacheng Feng^{*,†}

School of Chemistry and Chemical Engineering, Shandong University, Jinan 250100, People's Republic of China, Institute of Chemical Engineering and Material, Yantai University, Yantai 264005, People's Republic of China, Environment Research Institute, Shandong University, Jinan 250100, People's Republic of China, and Shandong Wanjie Group, Limited Liability Company, Zibo 255213, People's Republic of China

Received: April 21, 2009

The mechanisms of catalytic and thermal 1,2-rearrangement of (α -mercaptobenzyl)trimethylsilane were studied by using density functional theory (DFT) at the MP2/6-31+G(d,p)//B3LYP/6-31G(d) levels. The results show that (α -mercaptobenzyl)trimethylsilane rearranges to (benzylthio)trimethylsilane through a trimethylsilyl group migration from C to S atom via a transition state of pentacoordinate Si atom with or without radical initiators. The low reaction activation energy (15.1 kcal/mol) is responsible for the fast rearrangement in the presence of radical initiators. Both radical and nonradical thermal rearrangement mechanisms were suggested, and the radical mechanism dominates through its self-catalyzing. These results are consistent with the experiment results. The activation energy ($\Delta H_{\text{act}} = 15.1$ kcal/mol) for the rate-determining step within the self-catalytic cycle is low enough to make (trimethylsilylbenzyl)thiyl radical be a reasonable catalyst for the thermal rearrangement. The catalytic and thermal 1,2-rearrangement mechanisms of (α -mercaptobenzyl)trimethylsilane, especially the self-catalytic radical mechanism, were revealed for the first time. The comparison of the rearrangement mechanisms between (α -mercaptobenzyl)trimethylsilane and silylmethanethiol discloses the factors in determining the reaction mechanism of such kinds of mercaptoalkyl-functionalized organosilanes. The phenyl group is found to be favorable for the radical rearrangement, thus making (α -mercaptobenzyl)trimethylsilane instable.

1. Introduction

Mercapto-functionalized organosilanes and organosiloxanes are of great value in applications. As a kind of coupling agent with high coupling effectiveness, such silanes are broadly used as adhesion promoters in the rubber processing industry.^{1,2} In order to enhance the end-use properties of filled elastomers, research into the performance of mercapto-functionalized organosilanes is still being made.^{3–5} Owing to the high reactivity of the mercapto group, new types of silicone elastomers were developed. For example, based on the addition reaction of $-\text{SH}$ with $-\text{CH}=\text{CH}_2$ or $-\text{N}=\text{C}=\text{O}$, mercapto-functionalized organosiloxanes and aliphatically unsaturated organosiloxanes are cured together at room temperature in the presence of electromagnetic and particulate radiation, giving products as sealants and rubber articles.^{6,7} Initiated by copper(II), tin(IV), or mercury(I) salts, mercapto-functionalized organosilicon compounds including mercapto-functionalized organosilanes and organosiloxanes can be cured through the formation of disulfide bonds. The cured products vary from soft gels to elastomers to hard resins and are useful as molded articles, electrical encapsulants, and sealants.^{7,8}

Formation of organic films by self-assembly is a common approach for modification of a variety of metal surfaces. Recently, a number of reports of the self-assembly of (3-mercaptopropyl)trimethoxysilane on Au, Ag, or Pt surfaces or its application for three-dimensional film preparation on Au or Pt have been published.^{9–14} In the past few years, a convenient

methodology to prepare compact membranes with controlled thickness and structure was developed by combining the self-assembled monolayers of organosulfur compounds and the silica gel network based on alkoxy groups.^{13,15} (3-Mercaptopropyl)trimethoxysilane is comprised of two reactive functionalized groups, organosulfur and alkoxy groups. Due to its high reactivity, the mercapto group can be favorably modified to provide various functionalities. Thus, a mercapto-group-incorporated hybrid silica-based monolith was synthesized by incorporating mercapto groups into a silica precursor by sol-gel technology.^{16,17} The monolith was oxidized by hydrogen peroxide to produce sulfonic acid groups, implying huge potential for ion-exchange extraction applicability. They can be effectively applied to purify and enrich the target analytes in human urine.

However, mercapto-functionalized organosilanes are unstable under heating, ultraviolet radiation, or radical initiator. The instability is a disadvantage for their applications. Rearrangement is one of the characteristic reactions to cause the instability of mercapto-functionalized organosilanes. Early in the 1970s, Wright and West's research groups reported the first example of 1,2-rearrangement of mercaptoalkyl-functionalized organosilane. (α -Mercaptobenzyl)trimethylsilane rearranges spontaneously at 195 °C, or at 100 °C in the presence of catalytic amounts of radical initiator, to (benzylthio)trimethylsilane in high yield.^{18–20} It has been found that the thermal rearrangement of (α -mercaptobenzyl)trimethylsilane is not accelerated in the presence of polar solvent, suggesting that the transition state of the reaction is nonpolar.²⁰ Although it was assumed that this reaction might occur through catalysis by thermally generated thiyl radicals, no solid experimental evidence was found.²⁰ Does the thermal rearrangement occur via radical path? What

* Corresponding author, fdc@sdu.edu.cn.

[†] School of Chemistry and Chemical Engineering, Shandong University.

[‡] Institute of Chemical Engineering and Material, Yantai University.

[§] Environment Research Institute, Shandong University.

^{||} Shandong Wanjie Group, Limited Liability Company.

catalyzes the thermal rearrangement? If a thiyl radical catalyzes the thermal rearrangement, what kind of thiyl radical would it be? These questions, to our best knowledge, have not been answered experimentally or theoretically yet. Also, no further publications on the rearrangements of mercapto-functionalized organosilanes have been found after Wright and West's reports. Considering the wide range of applications of mercapto-functionalized organosilanes, in-depth understanding of their rearrangements and mechanisms is of practical value for the control and application of these compounds. It is also of importance for the development of mercapto-functionalized organosilane chemistry.

We recently studied the thermal 1,2-rearrangement of silyl-methanethiol $\text{H}_3\text{SiCH}_2\text{SH}$, which was used as a model of (α -mercaptobenzyl)trimethylsilane, by ab initio theory.²¹ The results show that the thermal rearrangement of silylmethanethiol occurs via nonradical path. That is to say, the reaction does not go on as Wright and West predicted. How about the thermal rearrangement of (α -mercaptobenzyl)trimethylsilane? Does it occur via radical path? Is there difference between the rearrangement mechanisms of the two mercaptoalkyl-functionalized organosilanes? If so, what is the difference? What leads to the difference? However, it is not easy to answer these questions experimentally.

In this paper, density functional theory studies on 1,2-rearrangement of (α -mercaptobenzyl)trimethylsilane is reported. It can be seen that the thermal rearrangement of (α -mercaptobenzyl)trimethylsilane is a radical reaction self-catalyzed by thermally generated thiyl radical, which is quite different from the case of the model compound silylmethanethiol. The factors determining the rearrangement mechanism of such kind of mercaptoalkyl-functionalized organosilane are revealed.

2. Computational Methods

The rearrangements of (α -mercaptobenzyl)trimethylsilane were studied by using density functional theory (DFT) at the MP2/6-31+G(d,p)//B3LYP/6-31G(d) levels.^{22–25} The molecules were optimized directly at the B3LYP/6-31G(d) level. The frequency calculations were performed at the same level. Only one imaginary frequency for each transition state could be found. UB3LYP was used for the radical species. Higher level energies were obtained using MP2/6-31+G(d,p) single-point calculations on the optimized structures. PMP2 energy was adopted for the radical species. The absolute energies, z_{pe} , enthalpies, and entropies of radical species are reported in Supporting Information. The nonradical paths were examined by intrinsic reaction coordinate (IRC) calculations at the B3LYP/6-31G(d) levels. The radical paths for the transition states **6**, **7**, and **9** were examined by IRC calculations at the UB3LYP/6-31G(d) levels. The other radical paths were not examined by IRC calculations due to the large number of atoms participating in bimolecular reactions. The IRC results are reported in Supporting Information. The radical transition states were verified by the vibrational modes of imaginary frequency. The stabilization energy of complexes was corrected taking into account the BSSE corrections. Natural bond orbital (NBO) analyses were performed at the (U)B3LYP/6-31G(d) level.²⁶ The Gaussian 03 series of programs were employed in all calculations.²⁷

3. Results and Discussion

3.1. Catalytic Rearrangement Initiated by Radical Initiators. The activation energy for the decomposition of azoisobutyronitrile (AIBN) is about 31 kcal/mol.²⁸ It may decompose at about 65–85 °C. So, it is easy for AIBN to initiate the rearrangement of (α -mercaptobenzyl)trimethylsilane (**1**) at

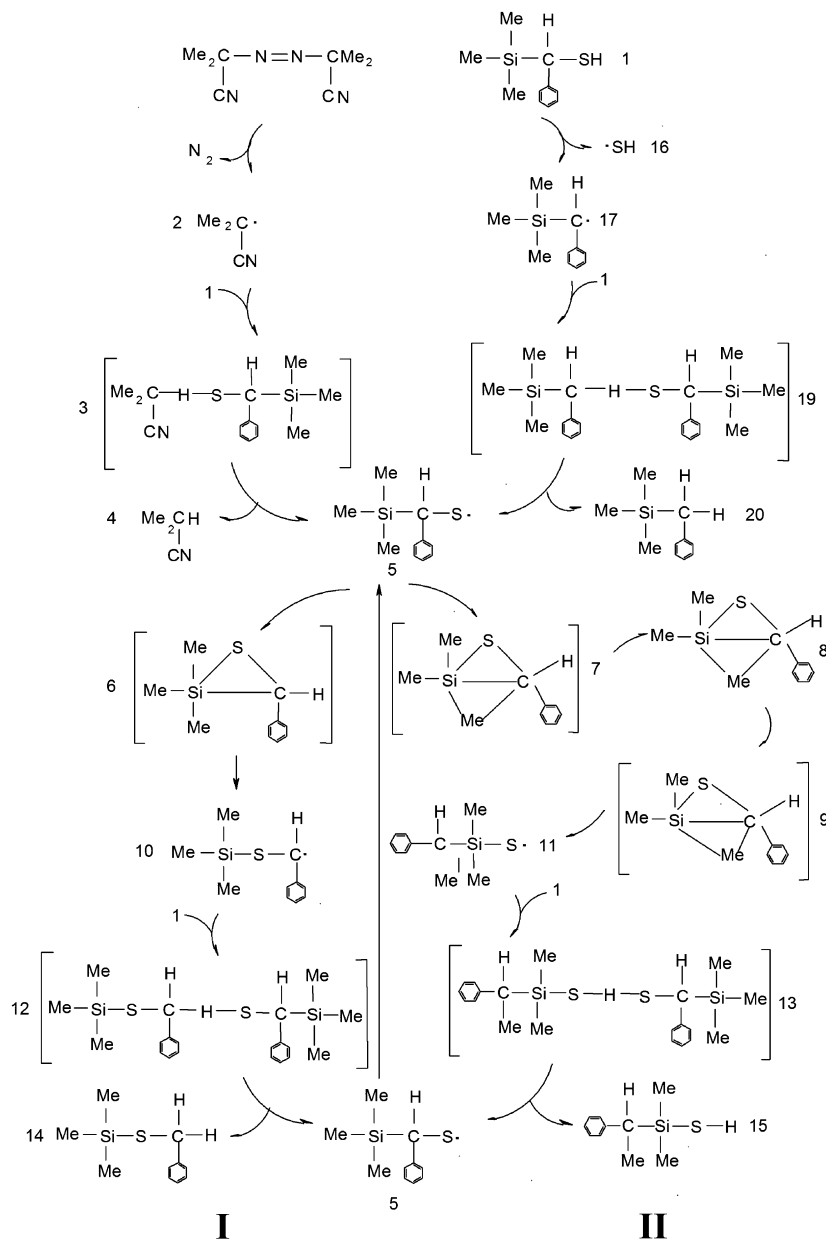
100 °C.²³ The mechanism is shown in Scheme 1(I).^{29,30} The geometries of transition state are given in Figure 1, along with the main vibrational modes of imaginary frequency.³¹

AIBN decomposes to give 2-cyano-2-propyl radical $\text{Me}_2(\text{CN})\text{C}^{\bullet}$ (**2**).²⁸ The catalytic rearrangement is initiated by the H-abstraction reaction of **2** from **1**, owing to the good susceptibility of sulfhydryl group to radical attack.³² As Figure 2 shows, this H-abstraction reaction has a little barrier of 0.5 kcal/mol. As shown in Figure 1, the main vibrational mode of the only one imaginary frequency of transition state **3** indicates that it involves the moving of a H atom between the mercapto S atom of **1** and the center C atom of **2**. So, it is believed that **3** is the transition state for the H-abstraction reaction, despite such a little barrier. The radical H-abstraction reactions with little barriers were also reported in other papers.^{33,34} The H-abstraction reaction is exothermic by 13.6 kcal/mol (Figure 2), yielding isobutyronitrile (**4**) and (trimethylsilylbenzyl)thiyl radical (**5**). The subsequent reaction is the rearrangement of **5**. It may occur via two paths, because two stationary points are located for the transition states of the rearrangement. One (**6**) is a three-membered ring, in which Si atom is pentacoordinate. As shown in Figure 1, the vibrational mode of the imaginary frequency of **6** indicates that it involves the dissociation of Si–C (benzyl) bond and the formation of Si–S bond. The IRC calculation results also verify that **6** is the transition state for the rearrangement of **5** to (trimethylsilylthio)benzyl radical (**10**) via 1,2-shift of trimethylsilyl group from C to S atom. The reaction is exothermic by 5.1 kcal/mol, and the barrier is 15.1 kcal/mol. The low barrier explains why the migration of silyl group is fast, as found in experiment. The calculation results provide a good confirmation of experimental prediction that the Si atom might become pentacoordinate in the rearrangement transition state.²⁰

The reaction of **5** rearranging to **10** via **6** could be explained more clearly by their structural parameters and the natural charges, which are shown in Figure 1. As compared with **5**, the Si–C (benzyl) distance in **6** increases from 1.981 to 2.199 Å, and at the same time the Si–S distance decreases to 2.428 Å. The structural changes lead to corresponding redistribution of electrons. For example, the negative charge of the benzyl C atom decreases by 0.267, and the positive charge of the Si atom decreases by 0.088. These changes could be mainly attributed to the weakened bonding interaction between the Si and the benzyl C atom. Owing to the weak bonding interaction between the S and Si atoms in **6**, the negative charge of the S atom increases by 0.168 (from 0.0705 in **5** to –0.0979 in **6**). As we know, the S atom is quite close to C atom in electronegativity and has a bigger atomic radius relative to the C atom. When **5** rearranges to **10**, the bonding of the Si atom with the C atom is displaced by that with the S atom, which makes the positive charge of the Si atom decrease by 0.193 (from 1.865 in **5** to 1.672 in **10**), and the negative charge of the S atom increase by 0.208 (from 0.0705 in **5** to –0.138 in **10**). In **10** the Si atom resumes to be tetraacoordinate. The electronic orbitals of the benzyl C atom at radical center adopt sp^2 hybrid, making the unpaired electron on the radical center delocalize to the phenyl group easily. It turns out that, despite being at the radical center, the negative charge (–0.351) of the benzyl C atom in **10** is less than that (–0.864) in **5**. Thus, **10** is 5.1 kcal/mol more stable than **5**.

The H-abstraction reaction by **10** from **1** follows the rearrangement of **5** to **10**, giving rearrangement product (benzylthio)trimethylsilane (**14**) and radical **5**. This step occurs via transition state **12** with a barrier of only 0.7 kcal/mol and is

SCHEME 1: Mechanism of Catalytic Rearrangement (I) and Radical Mechanism of Thermal Rearrangement (II)



exothermic ($\Delta H_{\text{react}} = -8.7$ kcal/mol). This is another example of radical H-abstraction reaction with little barrier. The transition state **12** could be confirmed by the main vibrational mode of the only one imaginary frequency, which involves the moving of a H atom between the mercapto S atom of **1** and the center C atom of **10**, as shown in Figure 1.

After the above step, as shown in Scheme 1(I), rearrangement of **1** is maintained via the cyclical reaction including the rearrangement of **5** and the H-abstraction reaction of the resultant **10** from **1**, leading to the product **14**, until **1** is used up. **14** is 13.8 kcal/mol more stable than **1** and is the thermodynamically preferred species at the equilibrium within the cycle. This is the reason for the high yield of the rearrangement.

In another path, **5** rearranges to (α -methylbenzyl)dimethylsilylthiyl radical (**11**) through two steps. In the first step, **5** rearranges to complex **8** via transition state **7**. As shown in Figure 2, the activation energy is 33.7 kcal/mol, and the reaction is endothermic by 32.3 kcal/mol. From the structural parameters shown in Figure 1 it can be seen that the bond between the S atom and the benzyl C atom is weakened in **7** as compared

with that in **5**, and a three-membered ring is formed among the S atom, the benzyl C atom, and the Si atom; meanwhile, a methyl group leaves the Si atom. The main vibrational mode of the imaginary frequency of **7** indicates that it involves the dissociation of the Si-C (methyl) bond. In complex **8**, the S-C (benzyl) bond is further weakened, while the S-Si bond is further strengthened; the methyl group is far away from the Si atom. In the second step, the complex **8** rearranges to **11** via transition state **9**. The activation energy is 17.3 kcal/mol, and the reaction is exothermic by 42.9 kcal/mol. As shown in Figure 1, the main vibrational mode of the imaginary frequency of **9** indicates that it involves the formation of the C(benzyl)-C(methyl) bond and the dissociation of the S-C(benzyl). The IRC calculation results also verify that the rearrangement of **5** to **11** is a two-step reaction. First, the S atom migrates from the benzyl C to Si atom and, meanwhile, a methyl group leaves the Si atom, then the methyl group approaches the benzyl C atom. The first step is the rate-determining step due to a higher barrier.

On comparison of the two paths of the rearrangement of **5**, it can be seen from Figure 2 that the barrier of **5** to **10** is 18.6

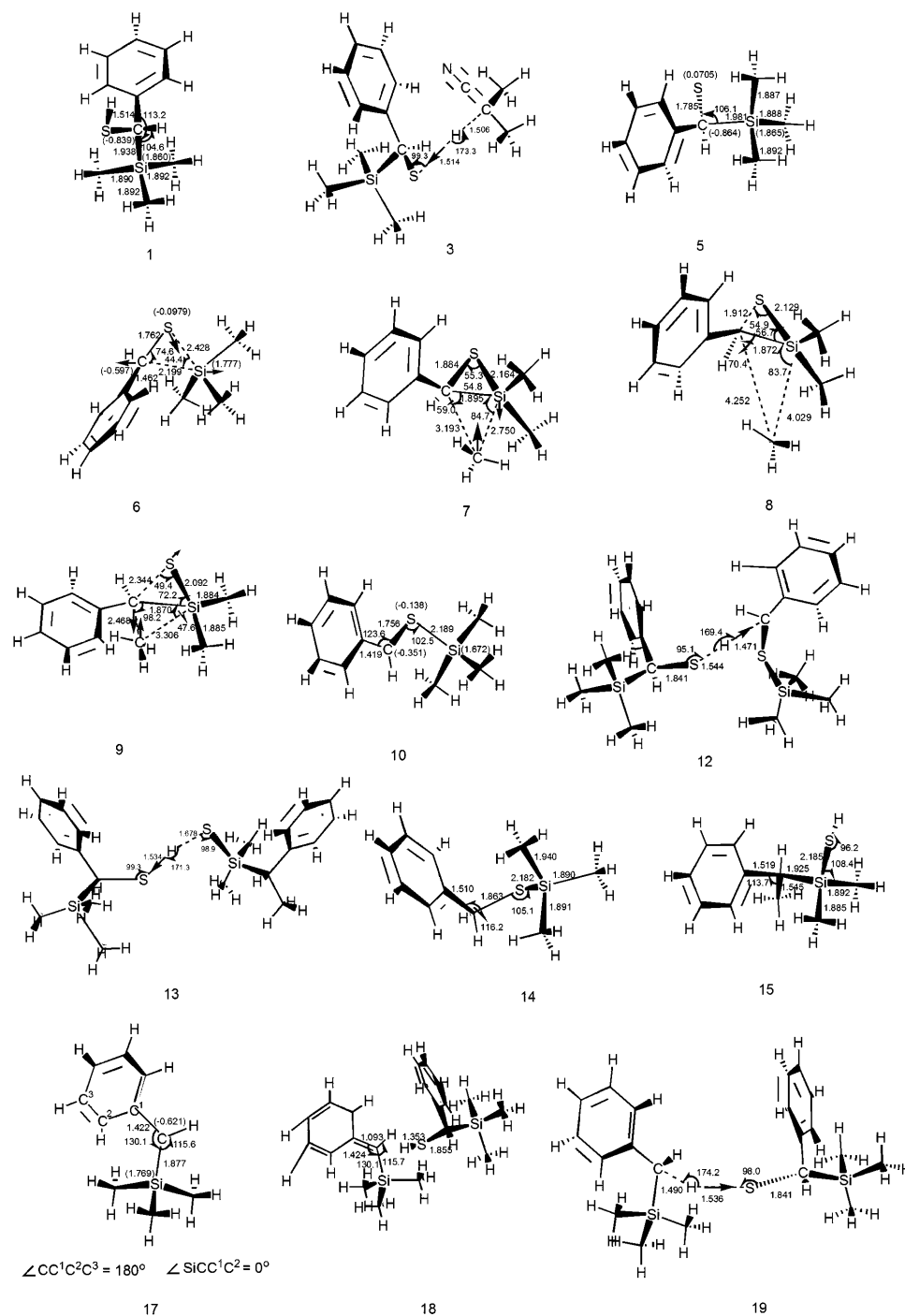


Figure 1. The B3LYP/6-31G(d) structural parameters (bond distance, angstroms; bond angle, degrees), and natural charges (in parentheses) of stationary points in Scheme 1. The arrows indicate the main vibrational modes of the imaginary frequencies in the transition states.

kcal/mol lower than that of **5** to **8**, which is the rate-determining step of **5** to **11**. As described above, **5** rearranges to **10** by a trimethylsilyl group migrating from the C to S atom, resulting in the dissociation of the Si–C(benzyl) bond, while **5** rearranges to **8** by a methyl group migrating from the Si to C atom, resulting in dissociation of the Si–C(methyl) bond. As far as the two Si–C bonds are concerned, the Si–C(benzyl) bond is a relatively weak one and might be broken easily. This is due to the well-known benzylic resonance, which can stabilize the reactive intermediate resulting from the dissociation of the bond.³⁵ The difference in strength between the two Si–C bonds can also be seen from the structural parameter of radical **5**. As shown in Figure 1, the Si–C(benzyl) bond distance is 1.981 Å, while the Si–C(methyl) bond distance is 1.892 Å. The differ-

ence in strength between the two Si–C bonds may be the main reason why the rearrangement of **5** to **11** is kinetically unfavorable as compared with that of **5** to **10**.

Following the rearrangement of **5** to **11**, the H-abstraction reaction by **11** from **1** needs to pass a low barrier of 2.5 kcal/mol in an exothermic reaction ($\Delta H_{\text{react}} = -4.7$ kcal/mol), yielding another rearrangement product, α -methylbenzyltrimethylsilylanethiol (**15**). **13** can be confirmed to be the transition state for the H-abstraction reaction by the main vibrational mode of the only one imaginary frequency in it, as shown in Figure 1. However, this path can be excluded because of the higher activation energy ($\Delta H_{\text{act}} = 33.7$ kcal/mol) of the rearrangement of **5** to **8**.

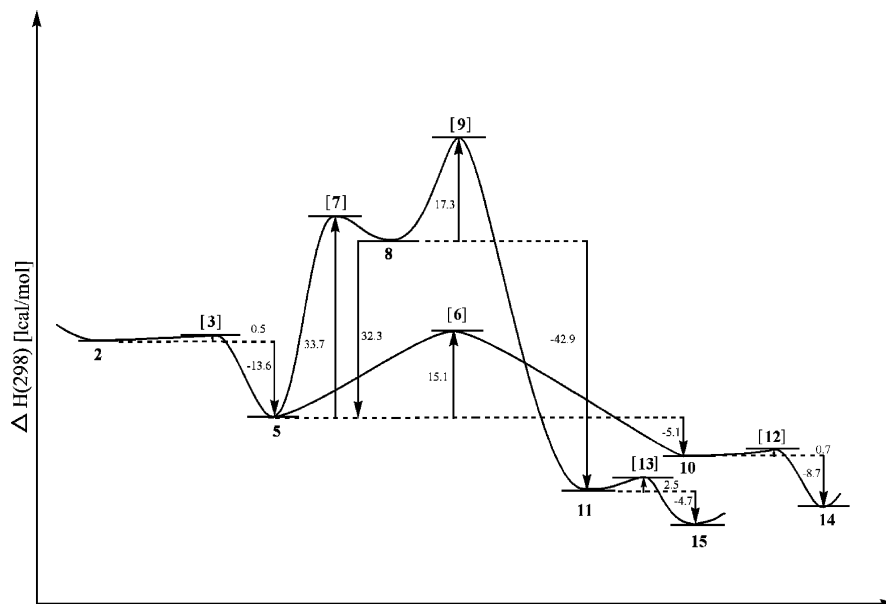


Figure 2. Enthalpy profile of mechanism of catalytic rearrangement initiated by radical initiators. The structures in brackets are transition states.

From the calculation results of the rearrangement of **1** to **14** initiated by radical initiators, it can be seen that after initiating by AIBN the reaction proceeds within a cycle. When a trimethylsilyl group migrates from C to S atom, the Si atom becomes pentacoordinate in the transition state. Requiring an activation energy of only 15.1 kcal/mol, the migration takes place fast. The rearrangement product **14** is 13.8 kcal/mol more stable than **1**. This is consistent with the experimental results that heating **1** for 37 min at 100 °C in the presence of AIBN gives 92% **14**.²⁰

3.2. Thermal Rearrangement. 3.2.1. Radical Mechanism.

It is difficult to initiate the rearrangement of **1** in the absence of radical initiators.^{20,32} Rearrangement of **1** does not occur until it is heated to 195 °C.²⁰ The radical mechanism of thermal rearrangement is shown in Scheme 1(II). The geometries of the transition state are shown in Figure 1, along with the main vibrational modes of the imaginary frequency. As shown in Scheme 1(II), the first step involves homolytic cleavage of the C–S bond, giving a HS radical (**16**) and a (trimethylsilyl)benzyl radical (**17**). However, it is a reaction without a transition state. As Figure 3 shows, the bond dissociation energy of the C–S bond is 67.5 kcal/mol, which is equal to reaction enthalpy. Despite the large bond dissociation energy, the homolytic cleavage of the C–S bond in **1** may be achieved at such a high temperature of 195 °C according to the report, and therefore thermal rearrangement of **1** would be initiated.²⁰ The following step is the H-abstraction reaction by **17** from **1**. First, an intermediate complex (**18**) is formed between **17** and **1**. As shown in Figure 3, the intermediate complex lies 4.4 kcal/mol below the two separated molecules. Then, the H-abstraction reaction occurs to give **5** and α -trimethylsilyltoluene (**20**) via transition state **19**. It is exothermic ($\Delta H_{\text{react}} = -7.9$ kcal/mol) and needs a little activation energy of 0.8 kcal/mol. As shown in Figure 1, the main vibrational mode of the only one imaginary frequency in **19** indicates that it is the transition state responsible for the above H-abstraction reaction involving the moving of a H atom from the mercapto S atom of **1** to the center C atom of **17**.

Once **5** is formed, the subsequent reaction may follow two paths, which is just like the cases of the catalytic rearrangement initiated by radical initiators, leading to rearrangement products

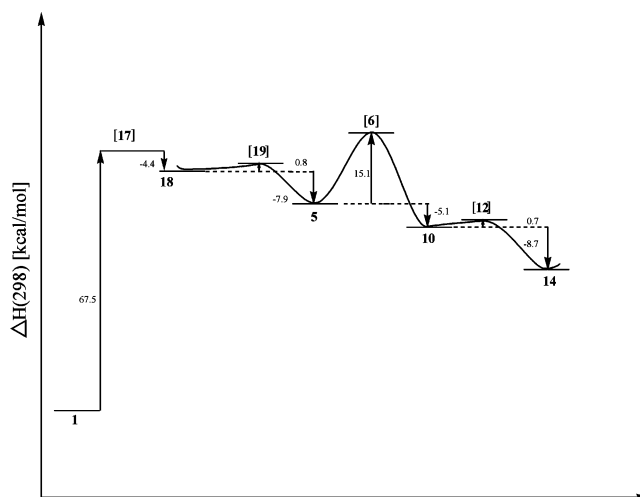


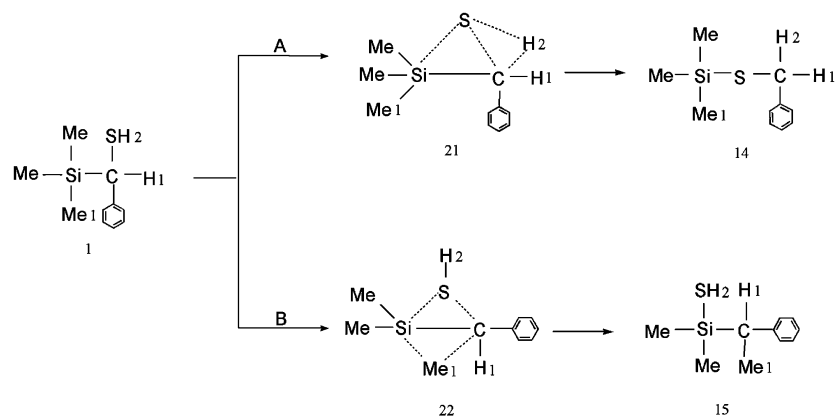
Figure 3. Enthalpy profile of radical mechanism of thermal rearrangement. The structures in brackets are transition states.

14 or **15**, respectively. The path giving **15** is disregarded because of the higher barrier of **5** rearranging to **11**.

By summarizing the radical mechanism of the thermal rearrangement of **1**, it can be seen that the homolytic cleavage of the C–S bond is the rate determining step. It occurs without a transition state, and the barrier is no less than 67.5 kcal/mol. However, the reaction could be initiated even though one or two molecules of **1** pass through the barrier, because the following reactions are self-catalyzed by **5**. As shown in Scheme 1(II), the formation of **5** causes the rearrangement to not go through the rate-determining step any more but to proceed within a cycle, including the rearrangement of **5** with a small barrier of 15.1 kcal/mol, and the H-abstraction reaction by the resultant radical **10** from **1** with a low barrier of 0.7 kcal/mol, yielding the final rearrangement product **14** and another **5**. Actually, **5** acts as a self-catalyzer in a like manner in the catalytic rearrangement initiated by radical initiators, as discussed in section 3.1. Thus, in the presence of catalytic amounts of AIBN, **1** rearranges spontaneously to **14** at 100 °C.

The proposed mechanism is consistent with the experimental results that 91% conversion to **14** occurs after 48 min when **1**

SCHEME 2: Nonradical Mechanism of Thermal Rearrangement



is heated to 195 °C in a sealed tube.²⁰ The above calculation results verify the experimental prediction that the rearrangement is catalyzed by thermally generated thiyl radicals. Here, the thiyl radical is confirmed to be the (trimethylsilylbenzyl)thiyl radical (5).

3.2.2. Nonradical Mechanism. Calculation results show that thermal 1,2-rearrangement of **1** may follow nonradical mechanisms. Two transition states are located for nonradical mechanisms, corresponding to two reaction paths. (Scheme 2). The geometries of transition states are shown in Figure 4.

In path A, a trimethylsilyl group migrates from the C to S atom, and the H atom (symbolized as H2 in Scheme 2) migrates from the S to C atom simultaneously via transition state **21**, leading to rearrangement product **14**. **21** is a double three-membered ring structure, in which the Si atom is pentacoordinate. As Figure 5 shows, the barrier for the reaction is 66.9 kcal/mol.

In radical mechanism, **5** rearranges to **10** via 1,2-shift of a trimethylsilyl group from C to S atom. On comparison with path A, it can be seen that both reactions involve the migration of trimethylsilyl group from the C to S atom and occur through transition states with pentacoordinate Si atom. The difference is that one is a radical reaction, while the other is a nonradical reaction. However, the barrier (66.9 kcal/mol) of the nonradical reaction is much higher than that (15.1 kcal/mol) of the radical one. Generally, this can be attributed to the higher activity of radical reaction. As for the migration of a trimethylsilyl group from the C to S atom, the radical reaction involves dissociation of the Si–C(benzyl) bond, while the nonradical reaction involves dissociation of both the Si–C (benzyl) bond and S–H bond. As can be seen from Figure 1, the Si–C(benzyl) distance in **5** is 1.981 Å, while the Si–C(benzyl) distance in **1** is 1.937 Å. This means that the Si–C(benzyl) bond in the radical reaction is a bit weaker than that involved in the nonradical reaction. With these points taken into consideration, it becomes better

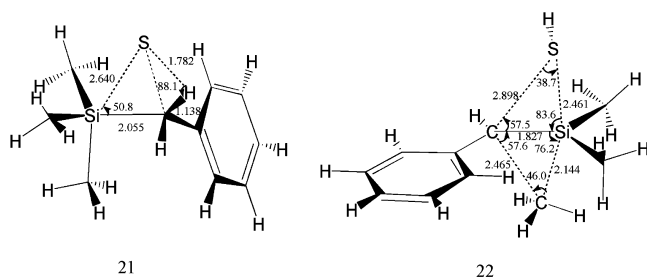


Figure 4. The B3LYP/6-31G(d) structural parameters (bond distance, angstroms; bond angle, degrees) of transition states in Scheme 2.

understood that the nonradical migration of the trimethylsilyl group from the C to S atom has to pass through a higher barrier than the radical one.

In path B, a mercapto group migrates from the C to Si atom, and a methyl group (symbolized as Me1 in Scheme 2) migrates from the Si to C atom simultaneously, giving rearrangement product **15**. Transition state **22** is also a double three-membered ring structure, in which the Si atom is also pentacoordinate. As can be seen from Figure 5, the barrier of the reaction is 77.8 kcal/mol, 10.9 kcal/mol higher than that of path A. In other words, the nonradical thermal rearrangement of **1** involving the migration of a trimethylsilyl group from the C to S atom is kinetically favored over the rearrangement involving the migration of a methyl group from the Si to C atom. As was stated above, the radical rearrangement involving the migration of a trimethylsilyl group from the C to S atom (**5** → **10**) is also kinetically favored over the rearrangement involving the migration of a methyl group from the Si to C atom (**5** → **11**). Namely, there is a similar result of the competition between the rearrangement involving the migration of a trimethylsilyl group from C to S atom and the rearrangement involving the migration of a methyl group from the Si to C atom, no matter if it follows the radical or nonradical mechanism. The reasons are also similar.

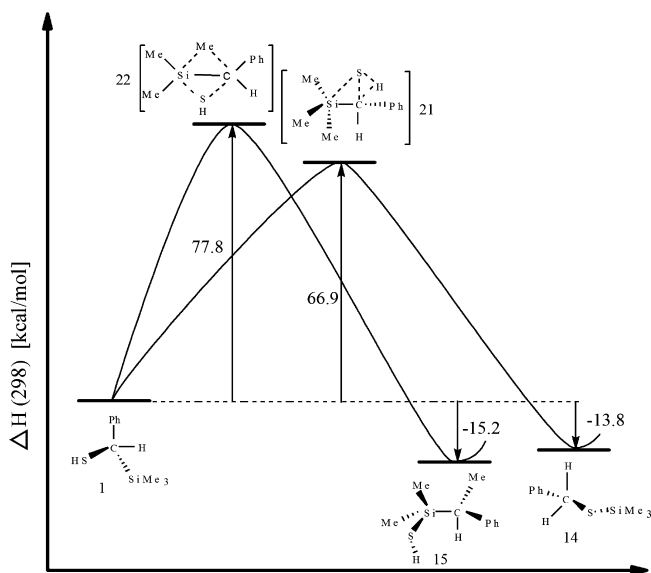
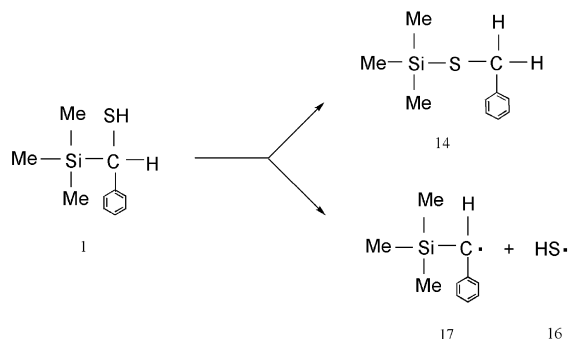


Figure 5. Enthalpy profile of a nonradical mechanism of thermal rearrangement. The structures in brackets are transition states.

SCHEME 3: Competition between Radical and Nonradical Mechanism of Thermal Rearrangement



It deserves to be mentioned that with regard to the nonradical path of a thermal 1,2-rearrangement, **1** and its model compound silylmethanethiol have similar results, that the rearrangement involving the migration of silyl group from C to S atom is kinetically favored over the rearrangement involving the migration of mercapto group from C to Si atom.²¹

On the basis of the above results, it can be concluded that, theoretically, the thermal rearrangement of **1** may follow a radical or nonradical mechanism. Which mechanism predominates? As Scheme 3 shows, it depends on the competition between the rate-determining step of the radical path and the favorable nonradical path.

The stability of the radical **17** resulting from the homolytic cleavage of the C–S bond controlled the rate-determining step of the radical mechanism. The more stable the resultant radical is, the lower the bond dissociation energy is. **17** is a benzyl radical, the benzyl C atom at the radical center is coplanar with the phenyl group, and the C–C (phenyl) distance is 1.422 Å, 0.092 Å shorter than that in **1**. This makes it easy for the uncoupled electron at the benzyl C atom to delocalize to the phenyl group. Moreover, the Si atom of the trimethylsilyl group is also coplanar with the benzyl group and thereby the benzyl radical acts as an electron donor and the trimethylsilyl group acts as an electron acceptor. This is the so-called $-T$ effect of the trimethylsilyl group due to the 3d orbital of the Si atom. This effect can be seen from the shortening of the Si–C (benzyl) distance (from 1.938 Å in **1** to 1.877 Å in **17**) and the decreasing of the positive charge of the Si atom (from 1.860 Å in **1** to 1.769 Å in **17**). Both effects, delocalization of the uncoupled electron to the phenyl group and the electron acceptability of the trimethylsilyl group, act to decentralize the uncoupled electron in **17**. Owing to the two effects, the negative charge of the benzyl C atom (-0.621) in **17** is even less than that (-0.839) in **1** despite being at the radical center. As a result, the stability of **17** is strengthened, and the bond dissociation energy of the C–S bond is lowered. Actually, the bond dissociation energy of the C–S bond is 67.5 kcal/mol, which is almost equal to the barrier (66.9 kcal/mol) of the favorable nonradical reaction. However, radical rearrangement is a self-catalyzed reaction. After **5** is formed, the rearrangement does not need to go through the rate-determining step any more, but proceeds within a cycle with a much lower barrier of 15.1 kcal/mol. In such a case, the nonradical paths can be excluded from the possible mechanisms of the thermal 1,2-rearrangement of **1**, and the thermal rearrangement of **1** follows the radical mechanism.

As for silylmethanethiol H_3SiCH_2SH , the silylmethyl radical $H_3SiC^{\bullet}(H_2)$ resulting from homolytic cleavage of the C–S bond would be very unstable due to the lack of substituent bonding with the center C atom to delocalize the uncoupled electron.

This means there would be a larger dissociation energy of the C–S bond. Thus, the radical path was not found for the thermal rearrangement of silylmethanethiol.²¹

It is logical to assume that in **1**, if the H atom bonding with the benzyl C atom is substituted by a group which can delocalize uncoupled electron, the substituted benzyl radical resulting from the homolytic cleavage of C–S bond would be more stable, and thereby the bond dissociation energy of the C–S bond would be lower. If so, the radical mechanism might be kinetically favored over the nonradical mechanism absolutely and the 1,2-rearrangement will occur more easily.

On the basis of the above understanding of the 1,2-rearrangement of **1**, it can be concluded that for mercaptoalkyl-functionalized organosilanes $R_3SiC(R_1R_2)SH$, thermal rearrangement may follow a radical or nonradical mechanism. In a radical reaction, the stability of the C radical ($R_3SiC^{\bullet}(R_1R_2)$) resulting from homolytic cleavage of the C–S bond controls the rate-determining step. The more stable the radical is, the more likely the radical mechanism predominates. Thus, those alkyl groups (R_1 and R_2) which can delocalize an unoccupied electron, and those substituted silyl groups (R_3Si) which can accept an electron would have a positive effect on a radical mechanism.

The effect of the alkyl groups (R_1 , R_2 , and R) on a nonradical mechanism works by influencing the strength of the Si–C bond. It is known that the bond energy of Si–C bond varies from 58.1 to 80.1 kcal/mol, depending on R_1 , R_2 , and R .³⁶ Generally speaking, the bigger the alkyl group, the smaller the bond energy of the Si–C bond. Those alkyl groups which act to weaken the Si–C bond would have a positive effect on the nonradical mechanism.

The alkyl and substituted silyl groups have a strong influence on the stability of mercaptoalkyl-functionalized organosilane $R_3SiC(R_1R_2)SH$ by having an effect on the mechanism of thermal rearrangement. For example, the phenyl group is unfavorable for the stability of **1** because it is favorable for the radical rearrangement. Further systematic studies about the effects of alkyl groups on the instability of such carbon-functionalized organosilicon compounds are being made.

4. Conclusions

Our calculations reveals the mechanisms of catalytic and thermal 1,2-rearrangement of **1**. The results show that the process involves radical cyclic reactions regardless of whether the radical initiator exists or not. In the presence of catalytic amounts of AIBN, **1** rearranges to **14** by a trimethylsilyl group migrating from C to S atom via a transition state with pentacoordinate Si atom. Requiring a low barrier of 15.1 kcal/mol, the catalytic rearrangement occurs fast. In the thermal rearrangement, **1** also rearranges to **14**, and the homolytic cleavage of C–S bond is the rate-determining step with a barrier no less than 67.5 kcal/mol. Once the homolytic cleavage is achieved by a few **1**, the rearrangement is initiated and proceeds easily through the catalysis of thermally generated **5**. The barrier of the formation of **5** is 5.9 kcal/mol. The barrier of the migration of a trimethylsilyl group from C to S atom is 15.1 kcal/mol, which is just like the cases of catalytic rearrangement initiated by radical initiators. The phenyl group is unfavorable for the stability of **1** because it is favorable for the radical rearrangement. The calculation results confirmed Wright and West's prediction that the thermal rearrangement occurs through catalysis by thermally generated thiyl radicals. Here the thiyl radical is found to be **5**. The proposed mechanism is consistent with the experimental results.

Acknowledgment. This work was supported by the Postdoctoral Scientific Research Item of Shandong Province (No.200603086), the National Natural Science Foundation of China (No. 20574043), the National Natural Science Foundation of China (Nos. 20903062, 20873074), 973 project of the Ministry of Science and Technology of China (No. 2009CB930103), and Natural Science Foundation of Shandong Province (No. Q2008B07).

Supporting Information Available: Tables containing standard orientation of all stationary points, IRC calculation results for nonradical mechanism of thermal rearrangement, IRC calculation results for radical mechanism of **5** to **10**, **5** to **8**, and **8** to **11**, and thermochemistry of radical species. This material is available free of charge via the Internet at <http://pubs.acs.org>.

References and Notes

- (1) Vanderbilt, Byron M.; Clayton, Robert E. US patent 3,350,345, 1967.
- (2) Fetterman, Miles Q. US patent 4,002,594, 1977.
- (3) Luginland, H. D.; Hasse, A. US patent 6,548,594 B2, 2003.
- (4) Deschler, U.; Krafczyk, R.; Korth, K.; Kiefer, I.; Horn, M. US patent 6,849,754 B2, 2005.
- (5) Chaves, A.; Pohl, E. R.; Kruse, R. W.; Gurovich, D. WO 2008/045262 A2, 2008.
- (6) Viventi, R. V. US Patent 3,816,282, 1974.
- (7) (a) Homan, G. R.; Lee, C. L. US patent 4,039,504, 1977. (b) Homan, G. R.; Lee, C. L. US patent 4,039,505, 1977. (c) Homan, G. R.; Toporcer, L. H. US patent 4,269, 991, 1981. (d) Homan, G. R.; Lee, C. L. US patent 4,070, 328, 1978. (e) Homan, G. R.; Lee, C. L. US patent 4,070,329, 1978. (f) Homan, G. R.; Lee, C. L. US patent 4,279,792, 1981.
- (8) Klosowski, J. M.; Snow, S. S. US patent 5,994,456, 1999.
- (9) Bryant, M. A.; Joa, S. L.; Pemberton, J. E. *Langmuir* **1992**, *8*, 753–756.
- (10) Blasini, D. R.; Tremont, R. J.; Batina, N.; Gonzalez, I.; Cabrera, C. R. *J. Electroanal. Chem.* **2003**, *540*, 45–52.
- (11) Thompson, W. R.; Cai, M.; Ho, M.; Pemberton, J. E. *Langmuir* **1997**, *13*, 2291–2302.
- (12) Bharathi, S.; Nogami, M.; Ikeda, S. *Langmuir* **2001**, *17*, 1–4.
- (13) Chen, X.; Wilson, G. S. *Langmuir* **2004**, *20*, 8762–8767.
- (14) Brito, R.; Rodriguez, V. A.; Figueroa, J.; Cabrera, C. R. *J. Electroanal. Chem.* **2002**, *520*, 47–52.
- (15) Niedziolka, J.; Palys, B.; Nowakowski, R.; Opalio, M. *J. Electroanal. Chem.* **2005**, *578*, 239–245.
- (16) Xie, C.; Hu, J.; Xiao, H.; Su, X.; Dong, J.; Tian, R.; He, Z.; Zou, H. *J. Sep. Sci.* **2005**, *28*, 751–756.
- (17) Li, X.; Lee, H. K. *J. Chromatogr., A* **2008**, *1195*, 78–84.
- (18) Wright, A.; West, R. *J. Am. Chem. Soc.* **1974**, *96*, 3214–3222.
- (19) Ling, D.; Boudjouk, P.; West, R. *J. Am. Chem. Soc.* **1972**, *94*, 4784–4785.
- (20) Wright, A.; West, R. *J. Am. Chem. Soc.* **1974**, *96*, 3222–3227.
- (21) Zhang, J.; Feng, S.; Feng, D.; Xie, J. *Int. J. Quantum Chem.* **2005**, *105*, 57–65.
- (22) Beck, A. D. *J. Chem. Phys.* **1993**, *98*, 1372–1377.
- (23) Beck, A. D. *Phys. Rev. A* **1988**, *38*, 3098–3100.
- (24) Perdew, J. P. *Phys. Rev. B* **1986**, *33*, 8822–8824.
- (25) Lee, C.; Yang, W.; Parr, R. G. *Phys. Rev. B* **1988**, *37*, 785–789.
- (26) (a) Carpenter, J. E.; Weinhold, F. *J. Mol. Struct.: THEOCHEM* **1988**, *169*, 41. (b) Carpenter, J. E. Ph.D. Thesis, University of Wisconsin, Madison, WI, 1987. (c) Foster, J. P.; Weinhold, F. *J. Am. Chem. Soc.* **1980**, *102*, 7211. (d) Reed, A. E.; Weinhold, F. *J. Chem. Phys.* **1983**, *78*, 4066. (e) Reed, A. E.; Weinhold, F. *J. Chem. Phys.* **1983**, *1736*. (f) Reed, A. E.; Weinstock, R. B.; Weinhold, F. *J. Chem. Phys.* **1985**, *83*, 735. (g) Reed, A. E.; Curtiss, L. A.; Weinhold, F. *Chem. Rev.* **1988**, *88*, 899.
- (27) Frisch, M. J.; Trucks, G. W.; Schlegel, H. B.; Scuseria, G. E.; Robb, M. A.; Cheeseman, J. R.; Montgomery, J. A., Jr.; Vreven, T.; Kudin, K. N.; Burant, J. C.; Millam, J. M.; Iyengar, S. S.; Tomasi, J.; Barone, V.; Mennucci, B.; Cossi, M.; Scalmani, G.; Rega, N.; Petersson, G. A.; Nakatsuji, H.; Hada, M.; Ehara, M.; Toyota, K.; Fukuda, R.; Hasegawa, J.; Ishida, M.; Nakajima, T.; Honda, Y.; Kitao, O.; Nakai, H.; Klene, M.; Li, X.; Knox, J. E.; Hratchian, H. P.; Cross, J. B.; Adamo, C.; Jaramillo, J.; Gomperts, R.; Stratmann, R. E.; Yazyev, O.; Austin, A. J.; Cammi, R.; Pomelli, C.; Ochterski, J. W.; Ayala, P. Y.; Morokuma, K.; Voth, G. A.; Salvador, P.; Dannenberg, J. J.; Zakrzewski, V. G.; Dapprich, S.; Daniels, A. D.; Strain, M. C.; Farkas, O.; Malick, D. K.; Rabuck, A. D.; Raghavachari, K.; Foresman, J. B.; Ortiz, J. V.; Cui, Q.; Baboul, A. G.; Clifford, S.; Cioslowski, J.; Stefanov, B. B.; Liu, G.; Liashenko, A.; Piskorz, P.; Komaromi, I.; Martin, R. L.; Fox, D. J.; Keith, T.; AlLaham, M. A.; Peng, C. Y.; Nanayakkara, A.; Challacombe, M.; Gill, P. M. W.; Johnson, B.; Chen, W.; Wong, M. W.; Gonzalez, C. Pople, J. A. *Gaussian 03, Revision B.05*; Gaussian, Inc.: Pittsburgh, PA, 2003.
- (28) Huang, R. L.; Goh, S. H.; Ong, S. H. *The Chemistry of Free Radical*; Translated by Mu, G. Z., Gan, L. Y., Chen, M. W.; Shanghai Science and Technology Press: Shanghai, China, 1974; Chapter 5, pp 61–62.
- (29) Engel, P. S.; Wu, H. F.; Smith, W. B. *Org. Lett.* **2001**, *3*, 3145–3148.
- (30) Hammond, G. S.; Wu, C. S.; Trapp, O. D.; Warkentin, J.; Keys, R. T. *J. Am. Chem. Soc.* **1960**, *82*, 5394–5399.
- (31) Su, M. D. *Chem. Phys. Lett.* **2003**, *374*, 385–391.
- (32) Colin, G. P.; Mary, S. F. *J. Am. Chem. Soc.* **1968**, *90*, 1928–1930.
- (33) Szori, M.; Fittschen, C.; Csizmadia, I. G.; Viskolcz, B. *J. Chem. Theory Comput.* **2006**, *2*, 1575–1586.
- (34) Henon, E.; Bohr, F. *Chem. Phys. Lett.* **2001**, *342*, 65–666.
- (35) (a) Laube, T.; Olah, G. A.; Bau, R. *J. Am. Chem. Soc.* **1997**, *119*, 3087–3092. (b) Lee, I.; Cho, J. K.; Kim, C. K. *Bull. Korean Chem. Soc.* **1991**, *12* (2), 182–188.
- (36) Du, Z. D.; Chen, J. H.; Bei, X. L.; Zhou, C. G. *Organo-silicon Chemistry*; High Education Press: Beijing, China, 1992; Chapter 1, pp 11–12.

JP903646M